

Isotopocule characterization of N₂O dynamics during simulated wastewater treatment under oxic and anoxic conditions

AZZAYA TUMENDELGER,^{1,2*} SAKAE TOYODA,³ NAOHIRO YOSHIDA,^{1,4} HIROSHI SHIOMI⁵ and RINA KOUNO^{5,6}

¹Department of Environmental Chemistry and Engineering, Tokyo Institute of Technology,
4259 Nagatsuta, Midori-ku, Yokohama 226-8502, Japan

²Institute of Chemistry and Chemical Technology, Mongolian Academy of Science, MAS 4th Building,
Peace Avenue, Bayanzurkh District, Ulaanbaatar 13330, Mongolia

³Department of Environmental Science and Technology, Tokyo Institute of Technology,
4259 Nagatsuta, Midori-ku, Yokohama 226-8502, Japan

⁴Earth-Life Science Institute, Tokyo Institute of Technology, Meguro-ku, Tokyo 152-8551, Japan

⁵Bureau of Sewerage, Tokyo Metropolitan Government, 2-8-1 Nishi-shinjyuku, Shinjyuku-ku, Tokyo 163-8001, Japan

⁶Bureau of Waterworks, Tokyo Metropolitan Government, 2-8-1 Nishi-shinjyuku, Shinjyuku-ku, Tokyo 163-8001, Japan

(Received August 24, 2014; Accepted August 23, 2015)

Isotopocule ratios of N₂O ($\delta^{15}\text{N}$, $\delta^{18}\text{O}$ and SP = ¹⁵N site preference within the linear N₂O molecule) are useful parameters to identify sources of this greenhouse gas and provide an insight into production and consumption mechanisms in a complex bacterial system. We measured isotopocule ratios of dissolved N₂O in simulated wastewater with activated sludge under variable conditions of key factors including dissolved oxygen (DO), carbon-to-nitrogen ratio (C/N ratio), mixed liquor suspended solid (MLSS), and water temperature in oxic and anoxic conditions. Under oxic condition, lower DO concentration causes greater N₂O accumulation. Observed low SP (−2.6 to +7.8‰ at 25°C and −7.2 to +9.2‰ at 18°C), which is unique to N₂O production pathway, and the relation of nitrogen isotope ratios between N₂O and its substrate (NH₄⁺) suggests that N₂O is produced mainly by NO₂[−] reduction by autotrophic nitrifiers (nitrifier-denitrification). The N₂O production mechanism in this condition was not altered by changes in DO of 0.5–3.0 mg L^{−1}. Under anoxic conditions, NO₂[−] reduction by denitrifying bacteria (heterotrophic denitrification) is the dominant contributor to N₂O production. Also, N₂O reduction to N₂ occurred simultaneously, as implied by isotopocule analysis. The C/N ratio had a negligible effect on the N₂O production mechanism. During anoxic N₂O decomposition experiment, a positive correlation between $\delta^{18}\text{O}$ and $\delta^{15}\text{N}^{\text{bulk}}$ (slope = 2.2) and between SP and ¹⁵N^{bulk} (slope = 0.9) of N₂O, which indicates the occurrence of N₂O reduction, were found. The N₂O reduction rate was increased by the high MLSS concentration. Moreover, isotopic enrichment factors (ϵ), which are specific to biological reaction, during N₂O reduction were estimated as $-9.5 \pm 1.0\text{‰}$ for $\delta^{15}\text{N}^{\text{bulk}}$, $-28.7 \pm 3.7\text{‰}$ for $\delta^{18}\text{O}$ and $-10.0 \pm 2.2\text{‰}$ for SP of N₂O.

Keywords: N₂O, isotopocule ratios, wastewater, N₂O reduction, oxic and anoxic condition

INTRODUCTION

Since the Industrial Revolution, concentrations of atmospheric nitrous oxide (N₂O), a powerful greenhouse gas, have increased by 20% from 271 ppb in pre-industrial era to 324 ppb at present as a result of anthropogenic activity (IPCC, 2007). It adversely affects the stratosphere, where it breaks down and acts as a catalyst in ozone layer destruction (Ravishankara *et al.*, 2009). Although it is not as abundant in the atmosphere as carbon dioxide (CO₂), its radiative forcing is about 300 times

greater on a per-molecule basis than that of CO₂ (IPCC, 2007). Different microbial pathways involved in biological nitrogen removal processes in wastewater treatment plants (WWTPs) can produce N₂O as well as more favorable gaseous product, N₂ (Colliver and Stephenson, 2000; Kimochi *et al.*, 1998). During nitrification, N₂O is produced from hydroxylamine (NH₂OH) as a byproduct of ammonium (NH₄⁺) oxidation to nitrite (NO₂[−]) by ammonia oxidizing bacteria. The concentration of dissolved oxygen (DO) should be maintained at an appropriate level because nitrifying bacteria require oxygen as an electron acceptor. During denitrification, N₂O is produced as an intermediate during nitrate (NO₃[−]) reduction to dinitrogen (N₂) by heterotrophic denitrifying bacteria in the absence of oxygen. Organics are used as electron donors in denitrification. Therefore, a sufficient amount of carbon

*Corresponding author (e-mail: azzaya@icct.mas.ac.mn; azzaya.usb@gmail.com)

is necessary to achieve effective nitrogen removal (Hanaki *et al.*, 1992; Itokawa *et al.*, 1996). Moreover, N_2O is producible through the nitrifier-denitrification pathway, which is the oxidation of NH_4^+ to NO_2^- followed by the reduction of NO_2^- to N_2O by autotrophic nitrifiers under insufficient oxygen conditions (Colliver and Stephenson, 2000; Wrage *et al.*, 2001).

Global N_2O emissions from WWTP are estimated as $0.22 \text{ Tg-N yr}^{-1}$, which accounts for approximately 2.8% of all anthropogenic sources (IPCC, 2007). To control and reduce N_2O emissions from WWTPs, key factors leading to N_2O production should be well managed during the biological nitrogen removal process. To date, key factors enhancing N_2O production were reported ambiguously in the literature as low DO, high NO_2^- accumulation or low carbon/nitrogen (C/N) ratios during denitrification (Itokawa *et al.*, 2001; Kampschreur *et al.*, 2008, 2009; Tallec *et al.*, 2006a; Wunderlin *et al.*, 2012) as well as short solid retention time (SRT) (Zheng *et al.*, 1994; Noda *et al.*, 2003). Therefore, identification of main N_2O production pathway and key factors leading to its production is necessary to develop wastewater treatment processes with low N_2O emission.

A few studies have provided information related to sources and production and consumption processes of N_2O using isotope ratios. By observations in full-scale WWTPs, nitrifier-denitrification was found to be the main contributor to N_2O production in an oxic tank, whereas NO_2^- reduction by heterotrophic denitrifier was the main source of N_2O in an anoxic tank (Townsend-Small *et al.*, 2011; Toyoda *et al.*, 2011a; Tumendelger *et al.*, 2014). Batch incubation experiments conducted under specific conditions demonstrated that nitrifier-denitrification dominantly produced N_2O in a multistep process of NH_4^+ oxidation (Wunderlin *et al.*, 2013). However, more isotopic studies must be done to elucidate the relative contributions from each N_2O production pathway and the occurrence of N_2O reduction in wastewater treatment operated under different conditions. For instance, no reports describe studies examining isotopic fractionation during N_2O reduction by activated sludge of a WWTP.

Natural abundance ratios of isotopocules (=molecular species that only differ in either the number or positions of isotopic substitutions, Coplen, 2011) of N_2O are useful tools for elucidating N_2O dynamics because they reflect the isotopic composition of the precursor materials (Kim and Graig, 1993; Yoshida *et al.*, 1989). In addition, analytical methods for determining the intramolecular ^{15}N distribution in the asymmetric N_2O molecule have been developed by Toyoda and Yoshida (1999) and Waechter *et al.* (2008). The ^{15}N -site preference, SP (difference in $^{15}\text{N}/^{14}\text{N}$ isotope ratio between central (α) and terminal (β) N), provided a new parameter to interpret N_2O production mechanisms and to estimate the global

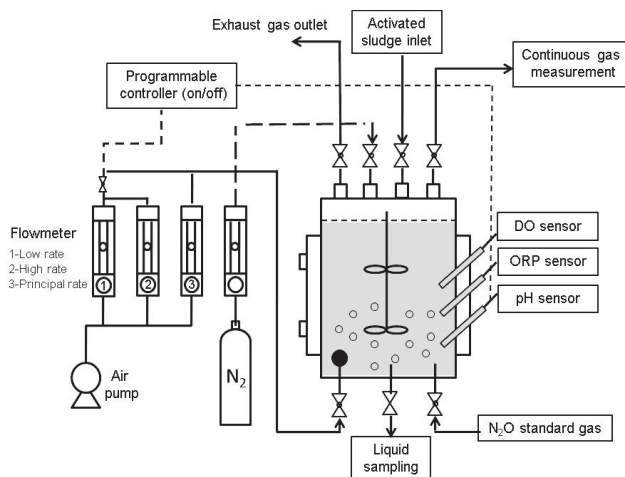


Fig. 1. Schematic of the laboratory-scale incubation reactor.

N_2O budget (Toyoda *et al.*, 2015; Yoshida and Toyoda, 2000). Earlier studies show that SP is independent of the substrate's isotopic signature, and unique value reflecting microbial production pathways (Sutka *et al.*, 2003, 2004, 2006; Toyoda *et al.*, 2005). For example, the SP of N_2O produced by NH_2OH oxidation is around +33‰, whereas the SP of N_2O produced by NO_2^- reduction is around 0‰. This significant difference enables SP to be used to distinguish production pathways in the environment. Therefore, isotopocule analysis can provide qualitative information that supplements the quantitative information produced by concentration analysis alone.

This study was conducted to elucidate the dependence of production and consumption mechanisms of N_2O during wastewater treatment on controlling factors such as DO, the C/N ratio, and water temperature. To accomplish this, we set up a series of oxic or anoxic batch-scale experiments with activated sewage sludge taken from a full-scale WWTP under variable experimental conditions. We first measured temporal changes in concentrations and isotope ratios of N_2O during its decomposition to reveal the effects of mixed liquor suspended solids (MLSS) on the N_2O reduction process and to estimate isotopic enrichment factors (ϵ) during N_2O reduction by activated sludge. Then we made time series measurements of concentrations and isotope ratios of N_2O and potential substrates (NH_4^+ and NO_3^-) to identify N_2O production pathways and to examine the occurrence of N_2O reduction.

EXPERIMENTAL

Lab-scale experimental reactor

A laboratory-scale incubation reactor with working volume of 30 L (Fig. 1) was filled with activated sludge

Table 1. Experimental conditions applied in oxic and anoxic batch tests

Experiment	Key controlling factors						
	DO ^a [mg L ⁻¹]	C/N ratio ^b [mgC mgN ⁻¹]		Nitrogen load ^c [mmolN L ⁻¹]		MLSS ^d [mg L ⁻¹]	
			[25°C]	[18°C]	[25°C]	[18°C]	[25°C]
Oxic							
N1	0.5	na		2.2	1.1	890	1380
N2	1.0	na		1.1	1.1	1058	1556
N3	2.0	na		1.5	1.4	912	1408
N4	3.0	na		1.0	1.4	898	1376
Anoxic							
D1	na	0.8 (0.68)	0.8 (0.68)	1.1	1.1	1234	1336
D2	na	1.2 (1.0)	1.3 (1.0)	1.1	1.1	1398	1132
D3	na	1.5 (1.4)	1.6 (1.4)	1.2	1.1	1230	1138
D4	na	2.4 (1.7)	2.0 (1.7)	1.0	1.2	1362	1376

na: not applicable.

^aSet point value around which actual value was kept constant.

^bMeasured initial value with target value in parentheses.

^cMeasured initial value. Target value was 1.4.

^dMeasured initial value. Target value was 1500.

taken from a municipal WWTP located in eastern Tokyo. The head space in the incubation vessel (about 7 L) was purged continuously with N₂ gas flow of about 4 L min⁻¹ using a flow controller to monitor the N₂O concentration. Air was supplied from the vessel bottom using three flow controllers to adjust the oxygen concentrations in oxic (nitrification) experiments. Measurements of DO, pH, and oxidation-reduction potential (ORP) were taken, respectively, using oxygen, pH, and ORP electrodes (DO-31P, HM-31P; TOA-DDK Corp., Tokyo, Japan). The pH was adjusted using sodium bicarbonate (NaHCO₃) at around 7.0 in an oxic experiment.

Batch incubation experiments

Each set of experiments was conducted at 25°C with activated sludge samples obtained in autumn (October–November, 2010) and replicated at 18°C with activated sludge samples obtained in winter (February, 2011) from biological oxic and anoxic reaction tanks at the WWTP. For N₂O decomposition experiments, activated sludge was collected in March, 2011.

N₂O decomposition experiments (R1 and R2) Activated sludge collected from the anoxic reaction tank was kept under anoxic conditions until all the NO₃⁻ and NO₂⁻ were completely consumed. Then it was diluted to 30 L with distilled water and was put into the incubation reactor. The experiments were conducted respectively at different MLSS concentrations: 189.2 mg L⁻¹ (R1) and 94.6 mg L⁻¹ (R2). After confirming that all DO was consumed and anoxic condition was established, the dissolved N₂O concentration was adjusted to approximately 30 μmol

L⁻¹ by bubbling with N₂O standard gas (1000 ppm) for about 1 hour at the rate of 4 L min⁻¹. Then the N₂O supply was stopped and experiments were started by adding organic carbon (100 mL of 22.2 g L⁻¹, CH₃COONa). Samples for dissolved N₂O analysis were collected immediately after bubbling with N₂O standard, 1 min after the addition of organic carbon (*t* = 0), *t* = 15 and 30 min. They were transferred into 125 ml glass vials (Maruemu Corp. Co. Ltd., Osaka, Japan), sterilized with 5 ml of saturated HgCl₂ solution to prevent microbial N₂O production or consumption, and then sealed with butyl rubber stoppers and aluminum caps with special care taken to exclude air bubbles. They were stored at 4°C and were analyzed within four weeks. Results confirmed that no significant change occurred in the dissolved concentration or isotopocule ratios of N₂O (data not shown).

Anoxic experiments (D1–D4) The experimental conditions of the anoxic N₂O production experiments are presented in Table 1. Activated sludge was collected from an anoxic reaction tank and was diluted to 30 L. Then it was put into the incubation reactor. After confirming that all DO was consumed and that anoxic condition was established, experiments were started by adding nitrate (KNO₃; 3.8 g-NL⁻¹) and organic carbon (CH₃COOH; 22.2 g L⁻¹) as substrates to adjust the initial NO₃⁻ concentration and C/N ratio. The water temperatures were set at 25°C and 18°C in autumn and winter experiments, respectively. Anoxic conditions were confirmed by the ORP measurement. They were negative at both temperatures. The pH levels were, respectively 7–9 and 7–8.5 at 25°C and 18°C. Experiments (D1–D4) were conducted under

Table 2. The $\delta^{15}\text{N}$ value of substrates (NH_4^+ and NO_3^-) applied in newly produced N_2O by two biological processes

Experiment	Time (min)	$\delta^{15}\text{N-NH}_4^+$		Experiment	Time (min)	$\delta^{15}\text{N-NO}_3^-$	
		[25°C]	[18°C]			[25°C]	[18°C]
Oxic				Anoxic			
N1	60	+7.3*	+4.2*	D1	60	+24.2**	+24.1**
N1	150	+10.6*	+10.2*	D1	150	+25.7**	+25.0**
N1	210	+13.8*	+14.0*	D1	210	+26.8**	+25.9**
N2	180	+35.2**	+18.9**	D2	180	+27.8**	+24.6**
N3	60	+8.1*	+7.3**	D3	60	+24.9**	+24.1**
N3	150	+26.0*	+16.1**	D3	150	+33.4**	+25.4**
N3	210	+68.3**	+25.3**	D3	210	+35.0**	+26.2**
N4	180	+40.1**	+18.3**	D4	60	+25.0*	+24.2**
				D4	150	+28.9*	+27.1**
				D4	210	+36.0*	+30.4**

*Measured value.

**Estimated value using Eq. (5) on the basis of measured concentrations and δ values in the experiments N1, N3 (for NH_4^+) and D4 (for NO_3^-).

different C/N ratios (C/N ratio of 0.68, 1.0, 1.4, and 1.7). For concentration analyses of dissolved inorganic nitrogen (DIN) species, water was sampled from the incubation chamber at 15 min intervals until 60 min passed, and then at 30 min intervals until 240 min. Sampling for concentration and isotopic analyses of dissolved N_2O was conducted less frequently for logistic reasons (e.g., available time for mass spectrometric analysis within the period for which collected samples can be stored without qualitative change), and sampling procedure was similar to those of N_2O decomposition experiment. Six samplings were conducted in experiments D1, D3 and D4 whereas two samplings for experiment D2, respectively. For isotopic analysis of NO_3^- , three samplings were done in experiment D4 (Table 2).

Oxic experiments (N1–N4) The experimental conditions of the oxic N_2O production experiments are presented in Table 1. Activated sludge was taken from an oxic reaction tank and was diluted to 30 L. Then it was put into the incubation reactor. The operating parameters (air flow, temperature and pH) were optimized to keep DO at a designated level before starting the experiment. Oxic conditions were confirmed by the ORP measurement. They were, respectively, +70–150 mV and about +200 mV at 25°C and 18°C. Experiments (N1–N4) were conducted under different oxygen concentrations (DO of 0.5, 1.0, 2.0 and 3.0 mg L⁻¹). Although we tried to control the N-loading and MLSS concentration at the target values, they were difficult to control in some cases probably because of inhomogeneity of the activated sludge (target value of N-load and MLSS are shown in the footnotes of Table 1). The experiments were started by adding a 100-ml solution of NH_4Cl (6 g-N L⁻¹) as a substrate so that the initial NH_4^+ concentration became the target value. The pH was initially adjusted by adding NaHCO_3 solution of >7.5 and

>7, respectively, at 25°C and 18°C. Sampling procedures and frequency for concentration analyses of DIN species were similar to those of anoxic experiments. Sampling procedures for concentration and isotopic analysis of dissolved N_2O are similar to those of anoxic experiments, and number of the collected samples were six or seven for experiments N1 and N3, and two for experiments N2 and N4. For isotopic measurement of NH_4^+ , samplings were done three times for experiments N1 and N3 (Table 2).

Analysis

The concentration of dissolved NH_4^+ was measured using a coulometric ammonia meter (MT-1; Central Kagaku Corp., Tokyo, Japan, and MM-60R; DKK-TOA Corp., Tokyo, Japan). The NO_3^- and NO_2^- were measured using an ion chromatograph equipped with a conductivity detector (DX-320; Dionex Corp., Osaka, Japan). Then N_2O analysis was performed using an isotope-ratio mass spectrometer (IRMS, MAT252; Thermo Fisher Scientific K.K., Yokohama, Japan) with an on-line analytical system comprising a glass-made gas extraction chamber in which the water is sparged with ultrapure helium, a stainless steel gas transfer line, a pre-concentration trap, and chemical traps for removal of H_2O and CO_2 (Fujii *et al.*, 2013; Yamagishi *et al.*, 2007).

Site-specific nitrogen isotope analysis in N_2O was conducted using ion detectors that had been modified for mass analysis of the N_2O fragment ions (NO^+), containing the N atoms in the central positions (α) of precursor N_2O molecules, whereas bulk (average) nitrogen and oxygen isotope ratios were determined from molecular ions (N_2O^+) (Toyoda and Yoshida, 1999). An aliquot of the water sample containing 1–5 nmol of N_2O was measured gravimetrically and introduced to the gas extraction cham-

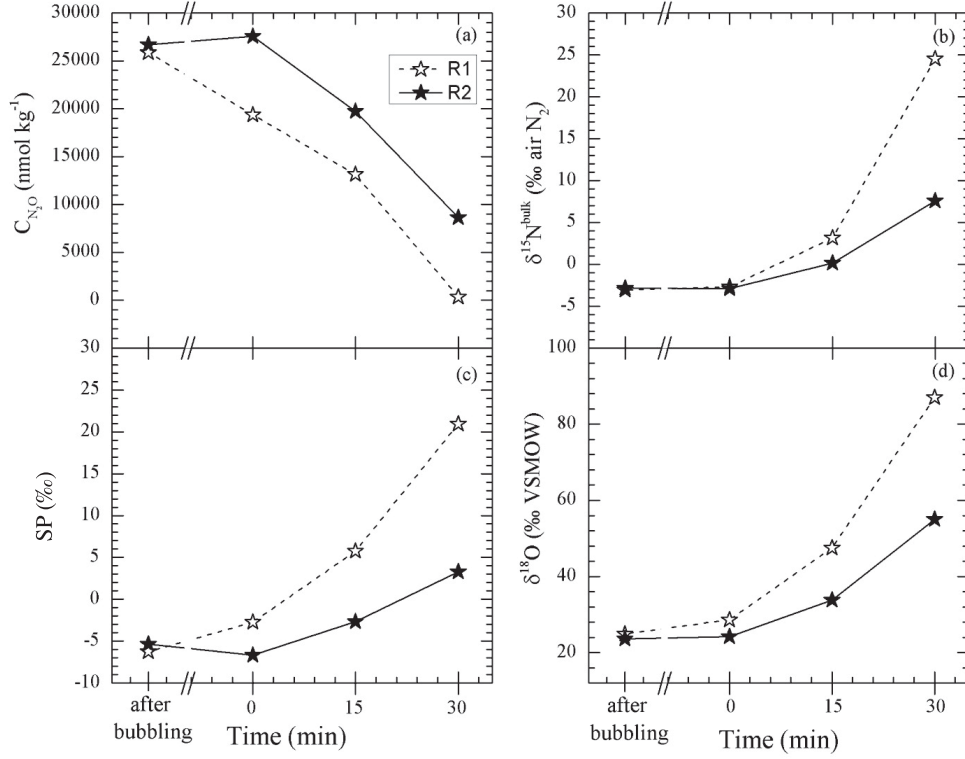


Fig. 2. Time courses of concentration (a) and isotopocule ratios ($\delta^{15}\text{N}^{\text{bulk}}$, SP, $\delta^{18}\text{O}$) (b–d) of N_2O in anoxic decomposition experiment at high (R1) and low (R2) MLSS concentrations. Data obtained immediately after bubbling with the standard N_2O gas and before adding organic carbon are shown left of the break in the horizontal axis.

ber with helium carrier gas. Pure N_2O gas (purity >99.999%; Showa Denko K.K., Japan) that had been calibrated previously with international standards was used as a laboratory standard for isotopocule ratios. The notation of the isotopocule ratio is the following.

$$\delta X = (R_{\text{sample}} - R_{\text{standard}}) / R_{\text{standard}} \quad (1)$$

In that equation, X is $^{15}\text{N}^{\alpha}$, $^{15}\text{N}^{\beta}$ or ^{18}O , and R denotes the $^{15}\text{N}/^{14}\text{N}$ ratios at the center or end N atoms in NNO molecules or $^{18}\text{O}/^{16}\text{O}$ ratio. Subscripts “sample” and “standard” respectively signify isotope ratios of the sample and the standard. The δ value is expressed as permil (‰). Standards are atmospheric N_2 for N and Vienna Standard Mean Ocean water (VSMOW) for O. In addition, instead of $\delta^{15}\text{N}^{\alpha}$ and $\delta^{15}\text{N}^{\beta}$, $\delta^{15}\text{N}^{\text{bulk}}$ and ^{15}N -site preference (SP) are defined as illustrative parameters for N_2O (Toyoda and Yoshida, 1999).

$$\delta^{15}\text{N}^{\text{bulk}} = (\delta^{15}\text{N}^{\alpha} + \delta^{15}\text{N}^{\beta}) / 2 \quad (2)$$

$$\text{SP} = \delta^{15}\text{N}^{\alpha} - \delta^{15}\text{N}^{\beta} \quad (3)$$

Measurement precision was typically better than 1% for

concentration, +0.1‰ for $\delta^{15}\text{N}^{\text{bulk}}$, +0.5‰ for $\delta^{18}\text{O}$, and better than +0.4‰ for $\delta^{15}\text{N}^{\alpha}$ and $\delta^{15}\text{N}^{\beta}$. The N_2O concentration was obtained simultaneously with the isotopocule ratios from the peak area of the major ions (masses 44 and 30 in molecular ion analysis and fragment ion analysis, respectively) measured in the sample water and standard gas (8.82 ppm N_2O in He).

If the N_2O reduction process is assumed to be negligible, the contributions of NO_2^- reduction (x) and NH_2OH oxidation ($1 - x$) to N_2O production are estimated using the SP value as presented below:

$$\text{SP}_{\text{sample}} = x \text{SP}_{\text{NO}_2^- \text{ reduction}} + (1 - x) \text{SP}_{\text{NH}_2\text{OH oxidation}} \quad (4)$$

Therein, $\text{SP}_{\text{NO}_2^- \text{ reduction}}$ and $\text{SP}_{\text{NH}_2\text{OH oxidation}}$, respectively, signify the SP values when N_2O is produced only by NO_2^- reduction and when N_2O is produced only by NH_2OH oxidation.

The $\delta^{15}\text{N}$ of NH_4^+ was measured using the diffusion method (Holmes *et al.*, 1998), where ammonium absorbed onto a glass fiber filter containing H_2SO_4 was converted to N_2 , and analyzed using an elemental analyzer-isotope ratio mass spectrometer (EA-IRMS) system (EA1110; Thermo Fisher Scientific K.K.). The $\delta^{15}\text{N}$ of NO_3^- was

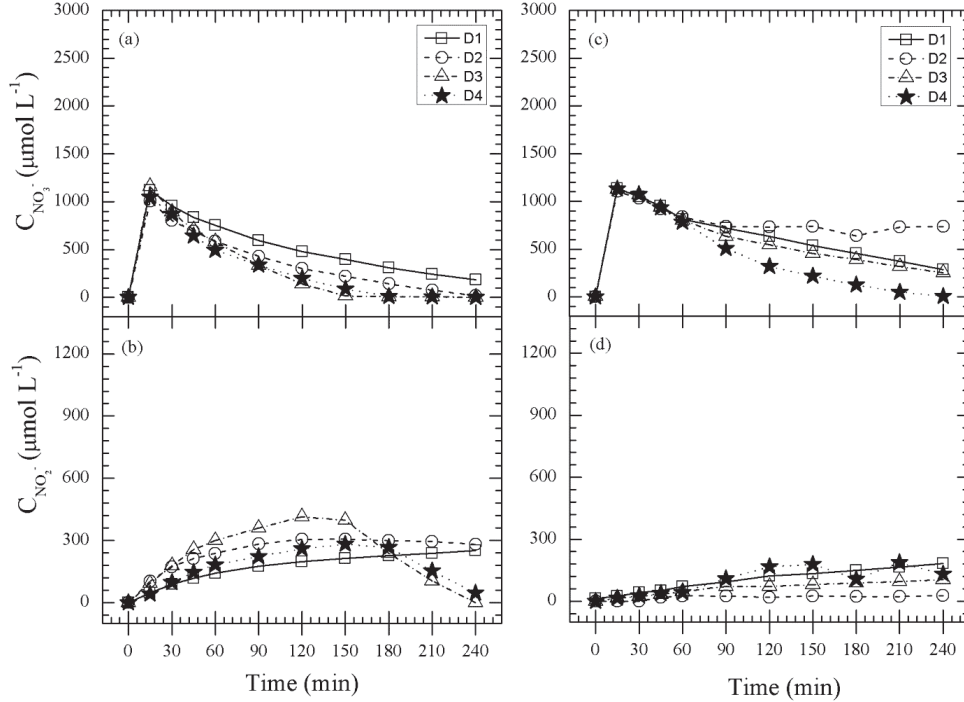


Fig. 3. Time course of the concentrations of NO_3^- and NO_2^- under anoxic conditions at 25°C (a, b) and 18°C (c, d).

measured using the denitrifier method (Casciotti *et al.*, 2002; Sigman *et al.*, 2001), where N_2O produced by *Pseudomonas aureofaciens* (NBRC 3521) from NO_3^- was analyzed as described above. The isotopic fractionation associated with possible incomplete diffusion or denitrification was canceled out by processing field samples and standards under identical conditions. The analytical precisions based on standard measurements were 0.3‰ and 0.2‰, respectively, for $\delta^{15}\text{N}$ of NH_4^+ and NO_3^- .

Isotopic discrimination during consumption of N_2O , NH_4 or NO_3^- in a closed system is defined as isotope enrichment factor, $\varepsilon(X)$ using a Rayleigh isotope fractionation model (Mariotti *et al.*, 1981).

$$\delta X = \delta_0 X + \varepsilon(X) \times \ln(C/C_0). \quad (5)$$

Therein, C denotes the concentration. Subscript 0 represents the initial value.

RESULTS

Effect of MLSS concentration on N_2O reduction

Results of the N_2O decomposition experiments R1 and R2 are presented in Fig. 2. The dissolved N_2O concentrations were 25880 nmol kg^{-1} and 26680 nmol kg^{-1} in experiments R1 and R2, respectively, after the bubbling of standard N_2O gas (Fig. 2a). In both experiments, the con-

centration of N_2O sharply decreased during the 30 min time course of the experiment. The reduction rate in experiment R1 (850 $\text{nmol kg}^{-1} \text{min}^{-1}$) with high MLSS concentration was higher than in R2 (533 $\text{nmol kg}^{-1} \text{min}^{-1}$). The isotopic ratios ($\delta^{15}\text{N}^{\text{bulk}}$, $\delta^{18}\text{O}$, and SP) of N_2O showed an intensive increment that ranged in $-2.7 - +24.5\text{‰}$ for $\delta^{15}\text{N}^{\text{bulk}}$, $+28.6 - +87.0\text{‰}$ for $\delta^{18}\text{O}$ and $-2.7 - +20.9\text{‰}$ for SP in experiment R1 whereas it was $-2.9 - +7.6\text{‰}$, $+24.2 - +55.0\text{‰}$ and $-6.7 - +3.3\text{‰}$, respectively in experiment R2 (Figs. 2b–d).

Effect of C/N ratio on N_2O production under anoxic conditions

The time courses of the NO_3^- and NO_2^- concentrations at 25°C and 18°C are portrayed in Fig. 3. The initial NO_3^- concentrations (1008–1159 $\mu\text{mol L}^{-1}$) in all experiments at both temperatures showed a monotonic decrease, which suggests the occurrence of heterotrophic denitrification (Figs. 3a and 3c). In experiments D1–D4, the NO_2^- concentration increased gradually from 0 to 212.4–397.5 $\mu\text{mol L}^{-1}$ until 150 min at 25°C. However, it was decreased to 40 $\mu\text{mol L}^{-1}$ at 240 min in experiments D3–D4. At 18°C, the NO_2^- concentrations in the experiments D1, D3, and D4 presented a slight increase along time courses, although it was almost constant in experiment D2 (Figs. 3b and 3d). The $\delta^{15}\text{N}$ values of NO_3^- at several timings in all experiments are presented in Table 2. The measurements of the $\delta^{15}\text{N}$ of NO_3^- were done

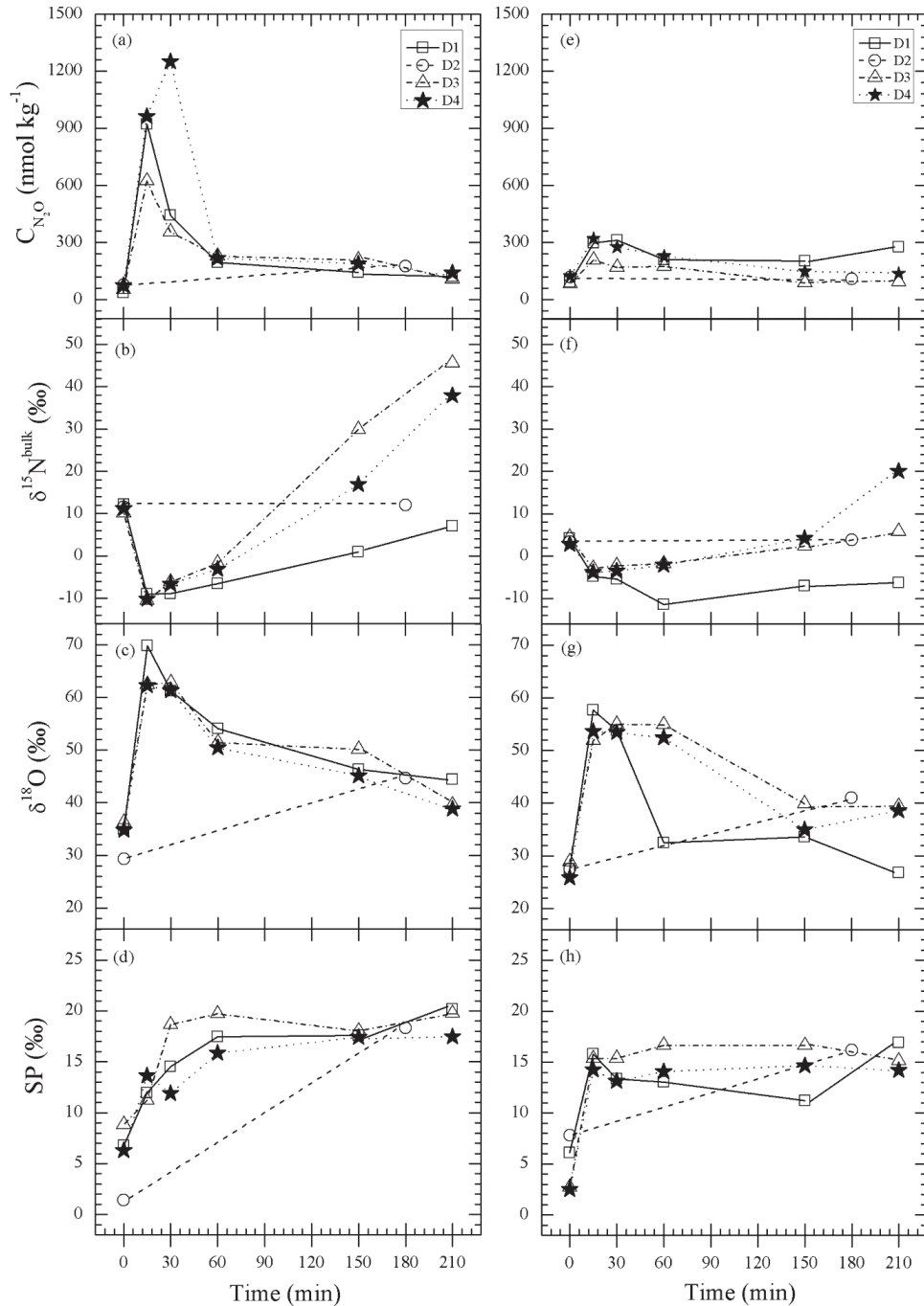


Fig. 4. Time course of the concentration and isotopocule ratios ($\delta^{15}\text{N}^{\text{bulk}}$, $\delta^{18}\text{O}$ and SP) of N_2O under anoxic condition (experiments D1–D4) at 25°C (a–d) and 18°C (e–h). The reference (control) experiment is D4 (stars). Effects of the C/N ratio were examined at these experiments.

only in the experiment D4 at 25°C, but we estimated the $\delta^{15}\text{N}$ values in other experiments using Eq. (5) based on measured NO_3^- concentrations and the parameters ($\delta_0^{15}\text{N} = +23.4\text{‰}$ and $\epsilon(^{15}\text{N}) = -2.3\text{‰}$) obtained from the fitting.

Figure 4 presents results of dissolved N_2O measure-

ments associated with factors controlling the production and consumption of N_2O . Experiments D1, D3, and D4 at both temperatures provide a time series of N_2O measurements showing a change in concentration and isotopocule ratios. The difference between D1, D3, and D4 was the C/N ratio. Unfortunately, we really do not

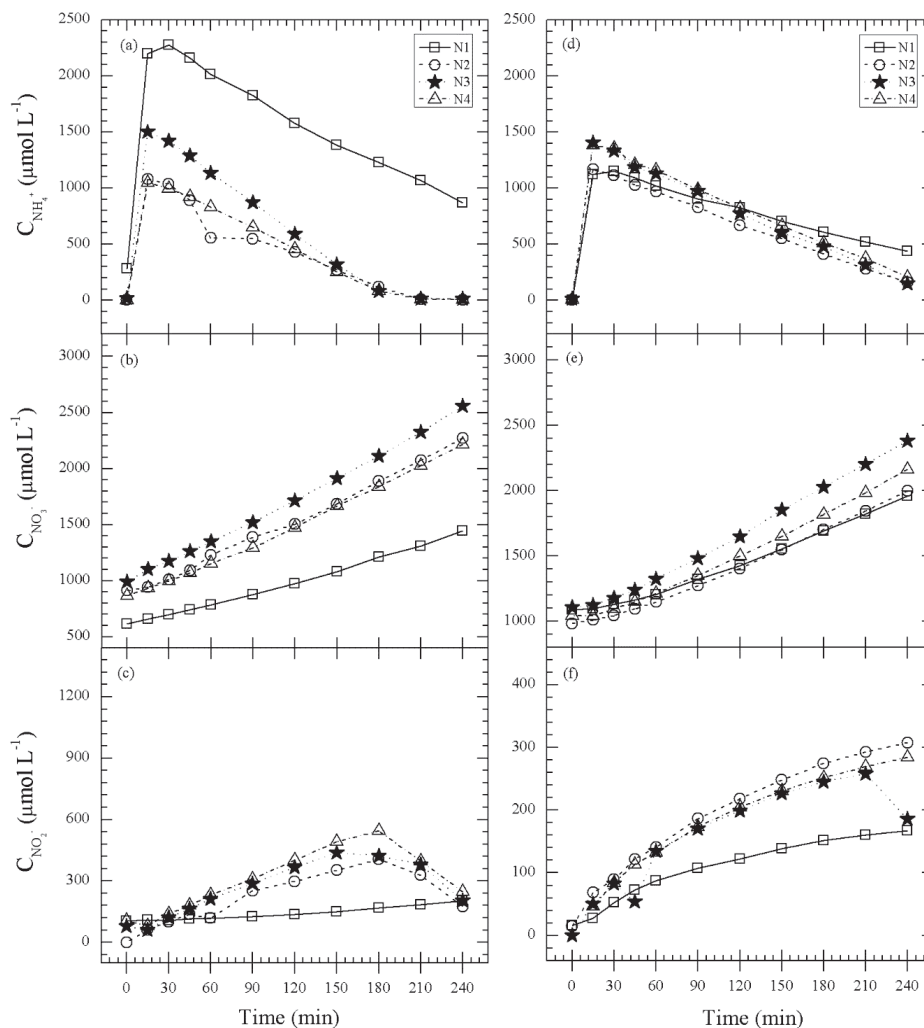


Fig. 5. Time course of the concentration of dissolved inorganic nitrogen species (NH_4^+ , NO_3^- and NO_2^-) under oxic conditions at 25°C (a–c) and 18°C (d–f).

know how concentrations and isotopocule ratios of N_2O were changed in experiment D2 because they were measured only at the beginning and then at the end of the time course.

At 25°C, the dissolved N_2O concentration increased as soon as the substrate was added. High N_2O concentrations were observed between 15 and 30 min, especially, reaching the maximum value of $920.5 \text{ nmol kg}^{-1}$ at the low C/N ratio of 0.8 (experiment D1) and $623.1 \text{ nmol kg}^{-1}$ at the middle C/N ratio of 1.5 (experiment D3). Subsequently, it became almost constant around 200 nmol kg^{-1} in all experiments after 60 min had passed. However, the highest N_2O ($1250.3 \text{ nmol kg}^{-1}$) was observed in experiment D4, which had the highest C/N ratio of 2.4 (Fig. 4a). The $\delta^{15}N^{\text{bulk}}$ of N_2O was increased in experiments D1, D3, and D4 when N_2O concentrations became almost stable after 60 min. In contrast, the $\delta^{18}O$ values in

these experiments were decreased slightly from +55‰ to +44‰ after a great increase in 15–30 min (Figs. 4b–d). The large SP values were observed as +17.5 – +20.2‰ for D1, +16.0 – +19.8‰ for D3 and D4, respectively.

At 18°C, the N_2O concentrations in experiments D1, D3 and D4 were increased slightly after substrate addition at 15 min. However, the concentration was about a quarter of the concentration observed at 25°C, and showed nearly stable patterns until the end of incubation. The $\delta^{15}N^{\text{bulk}}$ in experiments D1, D3, and D4 overlapped at 15 min, showing slightly greater (*ca.* –5‰) values compared to those observed at 25°C (*ca.* –10‰). They then increased to +5.8 – +20.0‰ except experiment D1 (Figs. 4e and 4f). The SP increased rapidly to +15.3 – +15.8‰ at 15 min in experiments D1 and D3. Thereafter, it fluctuated widely during incubation, although it became almost stable for experiment D4. Generally, the SP values at 18°C

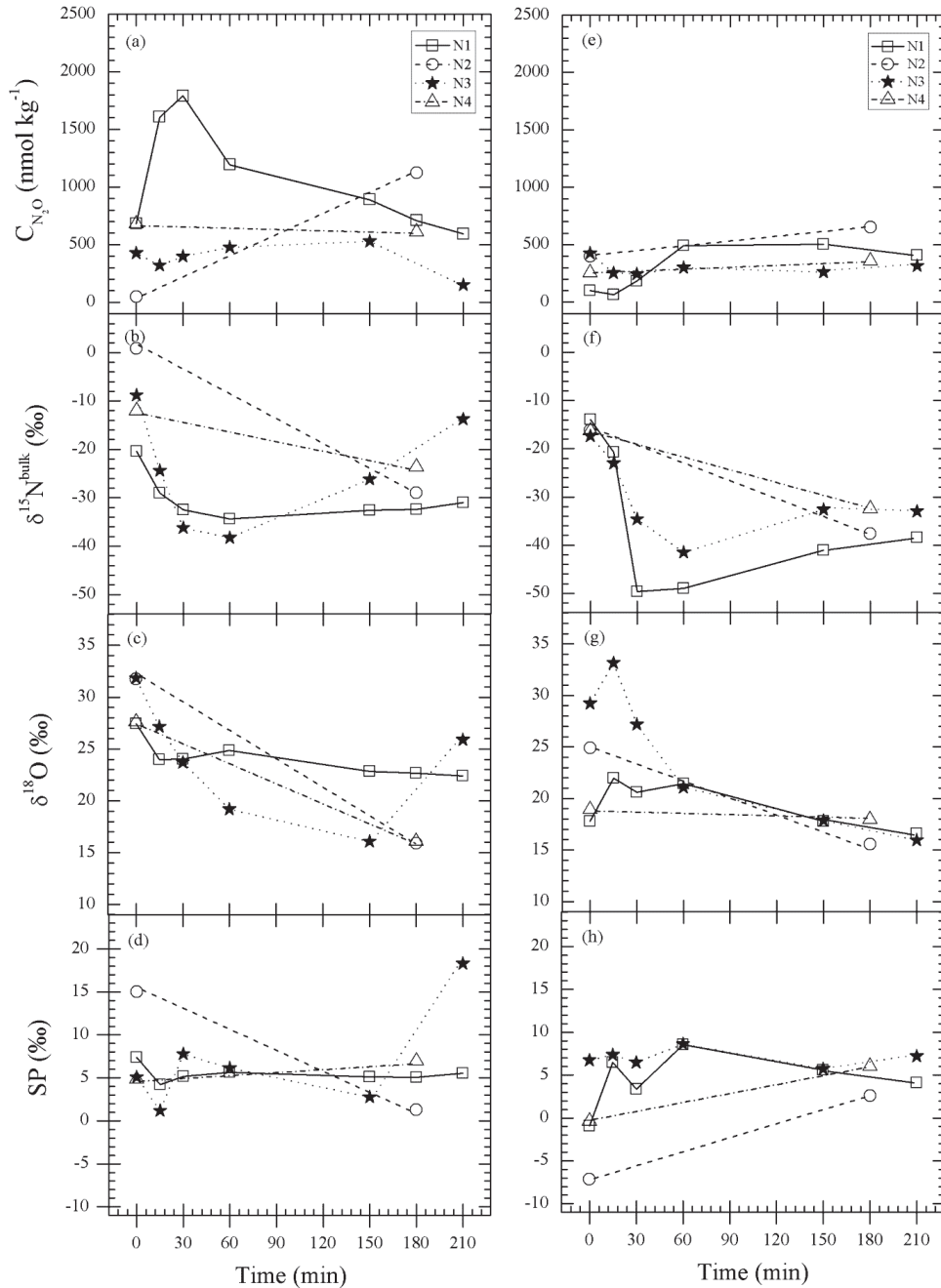


Fig. 6. Time course of the concentration and isotopocule ratios ($\delta^{15}N^{bulk}$, $\delta^{18}O$ and SP) of N_2O under oxic conditions (experiments N1–N4) at 25°C (a–d) and 18°C (e–h). The reference (control) experiment is N3 (stars). Effects of DO were examined at these experiments.

were slightly lower than those at 25°C (Fig. 4h). The $\delta^{18}O$ were high between 15 and 30 min followed by a decrease, but with large variations (Fig. 4g).

Effect of DO concentration on N_2O production under oxic conditions

Time course of the DIN concentrations in the oxic

experiments N1–N4 are portrayed in Fig. 5. The initial NH_4^+ concentrations (1078–2200 $\mu\text{mol L}^{-1}$) showed a monotonic decrease, whereas NO_2^- and NO_3^- concentrations are built up in all experiments. In experiments N2–N4 (DO of 1.0, 2.0 and 3.0 mg L^{-1}) at 25°C, the NO_2^- concentration was increased as high as 450 $\mu\text{mol L}^{-1}$. However, NO_2^- showed declines with continuous NO_3^-

increase at 180 min. The $\delta^{15}\text{N}$ values of NH_4^+ at several timing in all the experiments are presented in Table 2. Although we measured the $\delta^{15}\text{N}$ of NH_4^+ only in the experiments N1 (at 25°C and 18°C) and N3 at 60 min and 150 min (at 25°C), the data fit equation (5) quite well ($R^2 = 0.973$). Therefore, the $\delta^{15}\text{N}$ values for experiments N2 and N4 and those for N3 (at 18°C and at 210 min at 25°C) were estimated using Eq. (5), as in the case of $\delta^{15}\text{N}$ of NO_3^- in anoxic experiments. Fitting parameters used for the estimation were, respectively, +4.2‰ and -14.1‰ for $\delta_0^{15}\text{N}$ and $\epsilon(^{15}\text{N})$. These values are useful to estimate the $\delta^{15}\text{N}$ values of N_2O that might be produced from NH_4^+ (see Section “Discussion”).

The results of dissolved N_2O measurements associated with key factor of DO that affect N_2O production or consumption are shown in Fig. 6. Experiments N1 (DO of 0.5 mg L⁻¹) and N3 (DO of 2.0 mg L⁻¹) at both temperatures provide a full-time series of N_2O measurements showing the change in concentration and isotopocule ratios. At 25°C, the N_2O concentration increased to a maximum value of 1790 nmol kg⁻¹ around 15–30 min with a simultaneous decrease in $\delta^{15}\text{N}^{\text{bulk}}$ in experiment N1. Then the concentration decreased gradually until the end of incubation, whereas the $\delta^{15}\text{N}^{\text{bulk}}$, $\delta^{18}\text{O}$ and SP remained almost constant. In contrast, the N_2O concentration in experiment N3 was almost constant until 150 min (400–500 nmol kg⁻¹). However, it decreased with large increases in $\delta^{15}\text{N}^{\text{bulk}}$, $\delta^{18}\text{O}$, and SP of N_2O at 210 min (Figs. 6a, 6b, and 6d). At 18°C, a slight increase in N_2O concentration and a great decline in $\delta^{15}\text{N}^{\text{bulk}}$ were observed up to $t = 60$ min in experiment N1. They showed almost constant behavior. The SP of N_2O showed less variation. The N_2O concentration in experiment N3 was constant during the incubation. It was nearly two thirds of that observed in N1 between 60 and 210 min. The $\delta^{15}\text{N}^{\text{bulk}}$ varied widely, whereas SP was constant (+7.0 – +8.6‰) at 0–60 min after starting the experiment (Figs. 6e, 6f, and 6h).

The $\delta^{18}\text{O}$ of N_2O showed a great decline from +31.8‰ ($t = 0$) to +16.1‰ ($t = 150$ min) before a sudden increase at the end of the time course in experiment N3 at 25°C, although it increased slightly between $t = 0$ and 15 min, with a subsequent decrease that slows after 60 min at 18°C. In contrast, $\delta^{18}\text{O}$ - N_2O in experiment N1 was nearly constant around +23‰ after a small fluctuation at the beginning of incubation at high temperatures, although it was decreased slightly to +15.9‰ at 210 min at low temperatures (Figs. 6c and 6g).

DISCUSSION

N₂O reduction under anoxic conditions

The reduction rate of N_2O in experiment R1 (850 nmol kg⁻¹ min⁻¹) was higher than in R2 (533 nmol kg⁻¹ min⁻¹),

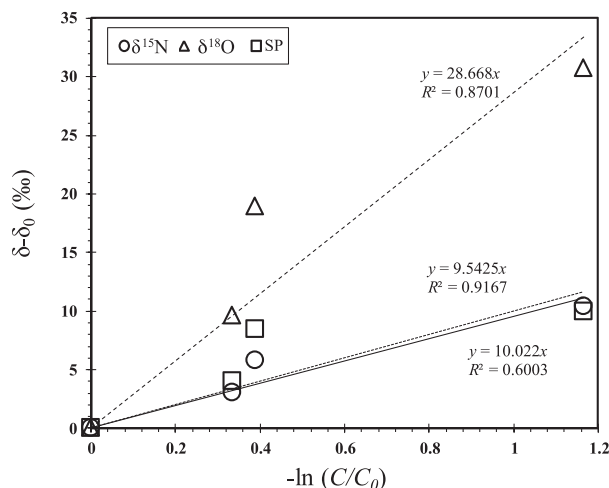


Fig. 7. Correlation between the dissolved N_2O concentration (C) and its isotopocule ratios (δ) during N_2O decomposition (Rayleigh plot). Subscript “0” denotes the value at $t = 0$ in Fig. 2. The data obtained at $t = 30$ min in experiment R1 is excluded (see text).

but the rate per unit MLSS was nearly the same, indicating that the microbes capable of N_2O reduction are distributed homogeneously in the suspended matter and that their activity is similar. The simultaneous increase in isotopocule ratios agrees with reports from pure culture incubation experiments of denitrifying bacteria in which residual N_2O becomes enriched in ^{15}N and ^{18}O during N_2O reduction (Ostrom *et al.*, 2007).

This report is the first of a study of the estimation of isotope enrichment factors for N_2O reduction (ϵ_R) during wastewater treatment applying Eq. (5). Fundamentally, the isotopic enrichment factor corresponds to the ratio of reaction rates for heavy-isotope-containing and light-isotope-containing molecules, during a simple unidirectional reaction or the rate limiting reaction of a multi-step reaction. The values of ϵ_R estimated using the combined dataset from both R1 and R2 experiments were $-9.5 \pm 1.0\text{‰}$ for the bulk N, $-28.7 \pm 3.7\text{‰}$ for the oxygen isotopes, and $-10.0 \pm 2.2\text{‰}$ for the SP of N_2O , although data obtained at $t = 30$ min in R1 was excluded because significant loss of N_2O by evasion to the gas phase was suspected (Fig. 7, Table 3). The ϵ_R of bulk ^{15}N and ^{18}O were within the range of reported values obtained in an oceanic environment ($-11.6 \pm 1.0\text{‰}$ for bulk N and $-30.5 \pm 3.2\text{‰}$ for ^{18}O) by Yamagishi *et al.* (2007). The ϵ_R of SP was slightly lower than the value estimated using pure cultures of denitrifier *Pseudomonas denitrificans* (-6.8‰) (Ostrom *et al.*, 2007). The reduction of N_2O prior to its emission to the atmosphere has the potential to result in changes in isotopocule ratios of N_2O that is often used to

Table 3. Reported and estimated enrichment factors for bacterial N₂O reduction process

Process	ϵ^{15} (N) (‰ air N ₂)	ϵ^{18} (O) (‰ VSMOW)	ϵ SP (‰ air N ₂)	Co-variation in isotopomer-isotopomer		Experimental condition/sample	References
				$\delta^{18}\text{O}/\delta^{15}\text{N}^{\text{bulk}}$	SP/ $\delta^{15}\text{N}^{\text{bulk}}$		
N ₂ O → N ₂	-26.0 ~ -5.0	nm	nm	nm	nm	<i>Ps. denitrificans</i>	Yoshida <i>et al.</i> (1984)
N ₂ O → N ₂	nm	-42.0 ~ -37.0	nm	nm	nm	<i>Ps. aeruginosa</i>	Yoshinari and Wahlen (1985)
N ₂ O → N ₂	-12.9	nm	nm	nm	nm	<i>Pa. denitrificans</i>	Barford <i>et al.</i> (1999)
N ₂ O → N ₂	-4.1	-10.9	-5.0	2.7	1.3	<i>Ps. slutzeri</i>	Ostrom <i>et al.</i> (2007)
N ₂ O → N ₂	-6.6	-15.0	-6.8	2.3	1.0	<i>Ps. denitrificans</i>	Ostrom <i>et al.</i> (2007)
N ₂ O → N ₂	-11.6 ± 1.0	-30.5 ± 3.2	-16.4	2.6	0.7	Eastern Tropical North Pacific	Yamagishi <i>et al.</i> (2007)
N ₂ O → N ₂	nm	nm	nm	2.4	1.2	Groundwater	Koba <i>et al.</i> (2009)
N ₂ O → N ₂	nm	nm	nm	~2.0	nm	Eastern Tropical North Pacific	Yoshinari <i>et al.</i> (1997)
N ₂ O → N ₂	nm	nm	nm	~3.0	nm	Arabian Sea	Yoshinari <i>et al.</i> (1997)
N ₂ O → N ₂	-9.5 ± 1.0	-28.7 ± 3.7	-10.0 ± 2.2	2.2	0.9	Wastewater incubation	This study

nm: not measured.

partition the production pathways. Therefore, the enrichment factors obtained in this study are expected to be useful parameters for further studies on N₂O reduction occurred in a complex bacterial system such as activated sludge.

We also examined the relation between $\delta^{18}\text{O}$ and $\delta^{15}\text{N}^{\text{bulk}}$ and between SP and $\delta^{15}\text{N}^{\text{bulk}}$ isotope fractionation as a potential means for identifying N₂O reduction. Observed linear relation between $\delta^{18}\text{O}$ and $\delta^{15}\text{N}^{\text{bulk}}$ using combined datasets at both R1 and R1 experiments is defined by slopes of 2.2, which is remarkably consistent with the slopes of 2.7 obtained in pure culture (Ostrom *et al.*, 2007) and slopes of 2.0 in marine environment (Yoshinari *et al.*, 1997). In other words, N₂O reductase has about a two-times-greater effect on oxygen isotopes than nitrogen isotopes. This might be used as a unique signature for this process. Furthermore, SP is known to increase in parallel with $\delta^{15}\text{N}$ with a slope of 1.2 ± 0.5 (Koba *et al.*, 2009). Positive linear correlation between SP and $\delta^{15}\text{N}$ of N₂O with slope of 0.9 ± 0.1 ($R^2 = 0.973$, $P < 0.05$), which conformed the slope acquired in groundwater (Koba *et al.*, 2009), was also observed in this study.

N₂O dynamics under anoxic conditions

Concentrations and isotopic signatures of DIN and N₂O

The monotonic decrease of initial NO₃⁻ concentrations (1008–1159 μmol L⁻¹) in all experiments at both temperatures suggests the occurrence of heterotrophic denitrification. Approximately 83.7–99.8% of NO₃⁻ was reduced to NO₂⁻ with slightly high reduction rate of 4.2–5.2 μmol L⁻¹ min⁻¹ in experiments D1–D4 (different C/N ratios) along the time course of incubation at 25°C, whereas a smaller fraction of NO₃⁻ is reduced (45–77.4%) with the rate of 1.6–3.9 μmol L⁻¹ min⁻¹ at 18°C (Figs. 3a and 3c).

As shown in Fig. 4, the dissolved N₂O concentration

was always higher than that of atmospheric equilibrium concentration (about 7.8 and 9.6 nmol kg⁻¹ at 25°C and 18°C, respectively) although the gas phase was purged continuously with N₂. This difference implies that N₂O production occurred at the range of C/N ratios tested in this study. At 25°C, the temporal accumulation of N₂O at low C/N ratio of 0.8 between 15 and 30 min agrees with studies by Chung and Chung (2000) and Hanaki *et al.* (1992) who found that limited availability of biodegradable organic carbon increases N₂O emissions in heterotrophic denitrification. However, the highest N₂O (1250.3 nmol kg⁻¹) was observed at the highest C/N ratio of 2.4, which might be caused the effects of other factors enhancing N₂O emission, such as NO₂⁻ accumulation or unbalanced activity of nitrogen reducing enzymes (Fig. 4a).

The $\delta^{15}\text{N}^{\text{bulk}}$ of N₂O was increased perhaps because of either N₂O production or reduction in experiments D1, D3, and D4 when N₂O concentrations became almost stable after 60 min. In contrast, the $\delta^{18}\text{O}$ values in these experiments were decreased slightly from +55‰ to +44‰, which are within the ranges of atmospheric values (+45 – +50‰, Yoshida and Toyoda, 2000) after a great increase in 15–30 min (Figs. 4b–d). The occurrence of N₂O reduction is suggested by observed large SP values (+17.5 – +20.2‰ for D1, +16.0 – +19.8‰ for D3 and D4) because N–O bond breakage during N₂O reduction enriches ¹⁵N in the alpha (α) position in the remaining N₂O molecules attributable to a primary kinetic isotope effect (i.e., the bonds of the light N₂O isotopocules break faster than those containing heavy isotopes) (Ostrom *et al.*, 2007). However, neither a temporal increase in SP values at the initial time ($t = 0$ –60 min) nor a monotonic increase in $\delta^{15}\text{N}^{\text{bulk}}$ throughout the incubation can give us full information explaining whether the reduction of N₂O alone occurred. Therefore, we attempted to check the occur-

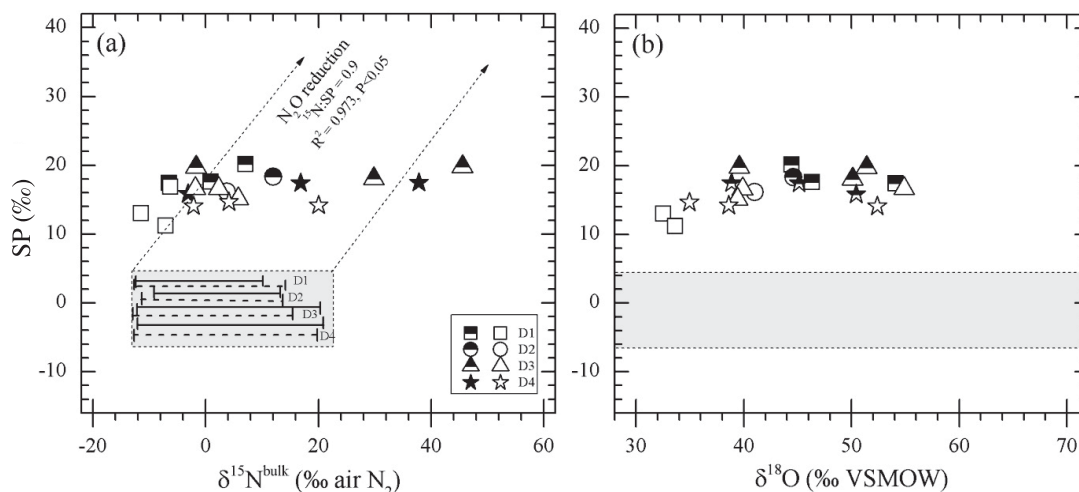


Fig. 8. Relation between SP and $\delta^{15}\text{N}^{\text{bulk}}$ and between SP and $\delta^{18}\text{O}$ of dissolved N_2O at 60–210 min during anoxic experiments at both 25°C and 18°C. Gray rectangles show overall ranges for N_2O produced by denitrification (NO_2^- reduction). The ranges of $\delta^{15}\text{N}^{\text{bulk}}$ for each experiment (D1–D4) were estimated using Eq. (5); they are shown by horizontal capped segments with solid (25°C) and dashed (18°C) lines (a). The SP of N_2O produced by NH_2OH oxidation was assigned as 29–37‰, whereas those by NO_2^- reduction were $-1.0 \pm 5.5\%$. In (b), only the expected ranges of SP are shown by horizontal belts. The N_2O produced in each experiment is shown with closed/half-closed (25°C) and open (18°C) symbols. The equation of reduction line is: $y = 0.9408x - 1.603$ (x denotes $\delta^{15}\text{N}^{\text{bulk}}$, and y denotes SP).

rence of N_2O reduction by the correlation between SP and $\delta^{18}\text{O}$ of N_2O . We found a poor correlation that might result from the simultaneous occurrence of N_2O production and reduction in this system. At 18°C, the N_2O concentrations in experiments D1, D3 and D4 were about a quarter of the concentration observed at 25°C, and showed nearly stable patterns until the end of incubation. In general, the SP values at 18°C were slightly lower than those at 25°C, which suggests that the rate of N_2O reduction was slow under low-temperature conditions (Fig. 4h). **Source-partitioning of N_2O** We infer that the N_2O net production (=production – consumption) and its emission from the water to the head space were balanced after 60 min because the N_2O concentration was stable in this system. Consequently, the isotopocule ratios after 60 min were regarded as values for N_2O net production.

In Figs. 8a and 8b, the data obtained at $t = 60$ min or later are shown, respectively, in SP- $\delta^{15}\text{N}^{\text{bulk}}$ and SP- $\delta^{18}\text{O}$ diagrams. Experiments D1–D4 were conducted under anoxic conditions. Therefore, N_2O should have been produced by heterotrophic denitrification as we expected. Reportedly SP of N_2O produced by the two pathways is independent of isotope ratios of the substrates (Sutka *et al.*, 2004, 2006; Toyoda *et al.*, 2005). We define the range of SP values for each pathway as $+33 \pm 4\%$ for NH_2OH oxidation and $-1.0 \pm 5.5\%$ for NO_2^- reduction according to estimations based on values from the literature (Toyoda *et al.*, 2011b and references therein). The range of SP values for N_2O produced by denitrification (i.e., nitrite

reduction) is shown by the vertical side of the gray rectangles in Figs. 8a and 8b. On the other hand, the range of $\delta^{15}\text{N}$ of N_2O produced by in each experiment can be estimated from $\delta^{15}\text{N}$ of substrate (NO_3^-) and isotopic enrichment factor for the pathway using the following equation.

$$\delta^{15}\text{N}_{\text{N}_2\text{O}} = \delta^{15}\text{N}_{\text{substrate}} + \varepsilon(^{15}\text{N})_{\text{substrate} \rightarrow \text{N}_2\text{O}} \quad (6)$$

The value of $\delta^{15}\text{N}-\text{NO}_3^-$ is taken from Table 2. The range of $\varepsilon(^{15}\text{N})_{\text{NO}_3^- \rightarrow \text{N}_2\text{O}}$ obtained by studies incubating pure culture of denitrifying bacteria under anaerobic conditions (–37 to –15‰, Toyoda *et al.*, 2011a). It is shown by a horizontal capped segment in the gray rectangle in Fig. 8a (solid and dashed lines respectively correspond to experiments conducted at 25°C and 18°C, respectively). As indicated by arrows in Fig. 8a, the $\delta^{15}\text{N}$ and SP are expected to show co-variation with a slope of 0.9 during N_2O reduction according to the results of experiments R1 and R2. In Fig. 8b, however, only the range of SP is shown for the same reason discussed in oxic experiments (see oxic experiment).

The measured SP of N_2O in experiments D1–D4 (+16‰ – +20‰ at 25°C and +11‰ – +17‰ at 18°C) with different C/N ratios were higher than the SP of N_2O produced by NO_2^- reduction (–1.0 to +5.5‰). Consequently, the measured N_2O cannot be explained solely by the NO_2^- reduction. In Fig. 8a, the observed data are distributed in the region located upward and slightly rightward of the

gray box. They are bounded by the slanted arrows drawn from the box, which strongly suggests the occurrence of simultaneous N_2O production by NO_2^- reduction and N_2O reduction to N_2 . In summary, results show that N_2O was produced mainly by heterotrophic denitrification. It was then partially reduced to dinitrogen gas in all experiments tested under various C/N ratios at different temperatures. The difference in C/N ratios had no effect on the production pathway.

N₂O dynamics under oxic conditions

Concentrations and isotopic signatures of DIN and N₂O
Based on monotonic decrease of initial NH_4^+ concentrations following to increments of NO_2^- and NO_3^- concentrations, we found that approximately 98.3–99.1% of initial NH_4^+ was converted into NO_2^- and NO_3^- by the end of incubation with the NH_4^+ oxidation rate of 5.3–7.6 $\mu\text{mol L}^{-1} \text{min}^{-1}$ in experiments N2–N4 (DO of 1.0, 2.0 and 3.0 mg L^{-1}) at 25°C (Fig. 5). The NO_2^- concentration in these experiments was high as 450 $\mu\text{mol L}^{-1}$. Such an accumulation of NO_2^- during the oxidation of NH_4^+ by activated sludge has also been described in reports of previous studies (Itokawa *et al.*, 2001; Kampschreur *et al.*, 2008). However, NO_2^- showed declines with continuous NO_3^- increase at 180 min, which indicates NO_2^- oxidation to NO_3^- by nitrifiers. In contrast, the fraction of NH_4^+ oxidized was low in experiment N1 with low DO (0.5 mg L^{-1}). It was about 60.5% with the rate of 5.9 $\mu\text{mol L}^{-1} \text{min}^{-1}$ at 25°C, whereas it was 60.8% with the rate of 3.0 $\mu\text{mol L}^{-1} \text{min}^{-1}$ at 18°C, which indicates that NH_4^+ oxidation is affected by the insufficient amount of oxygen concentration. This trend confirms the presence of ammonia-oxidizing bacteria (AOB) and nitrite oxidizing bacteria (NOB). Moreover, it indicates no significant heterotrophic activity. The NH_4^+ oxidation rates at 25°C were slightly higher than those of 18°C, indicating that AOB can be more active in warmer conditions.

Because the liquid phase and the gas phase were purged continuously with air and N_2 , respectively, the dissolved N_2O concentration was controlled not only by the rates of production and reduction by microbes, but also by the rate of diffusion to the gas phase. Nevertheless, it was always higher than the concentration expected under atmospheric equilibrium (approximately 7.8 and 9.6 nmol kg^{-1} at 25°C and 18°C, respectively (Weiss and Price, 1980)), indicating that significant N_2O production occurred at the range of DO tested in this study (Fig. 6a). At 25°C, the N_2O concentration increased with simultaneous decrease in $\delta^{15}\text{N}^{\text{bulk}}$ around 15–30 min in experiment N1 with the lowest DO condition (0.5 mg L^{-1}). The accumulation of N_2O in this low condition means a higher N_2O production rate relative to the rate of diffusive loss, which is consistent with previous works reporting that lower DO concentrations engender higher N_2O emissions

during nitrification (Kampschreur *et al.*, 2008; Tallec *et al.*, 2006). The decrease in $\delta^{15}\text{N}^{\text{bulk}}$ during the N_2O increasing phase is explained by addition of isotopically light N_2O produced by nitrification, as described later. Thereafter, the concentration decreased gradually until the end of incubation when the isotopocule ratios of N_2O remained almost constant, which suggest that the accumulated N_2O was emitted gradually to the gas phase with only a marginal isotope effect (Inoue and Mook, 1994). For experiment N3 with high DO concentration, almost constant N_2O concentration until 150 min implies that the N_2O production and its emission to the gas phase were balanced. However, it decreased with large increases in $\delta^{15}\text{N}^{\text{bulk}}$, $\delta^{18}\text{O}$, and SP of N_2O at the end of incubation (Figs. 6a–d), which might be caused by occurrence of N_2O reduction by denitrifiers locally existed in suspended matter. In experiment N3, N_2O concentrations were low compared to those of experiment N1 in which the DO concentration was lower than in experiment N3. This result is consistent with findings by Zheng *et al.* (1994) who reported that the high DO level can minimize N_2O production from nitrification.

Results of experiment N1 show that the N_2O concentration was lower at 18°C than at 25°C by a factor of two or three. This would have been caused not only by the temperature difference but also by unexpectedly high N-loading at 25°C (Figs. 5a and 5d). Although the difference was not as large as in the case of N1, a similar temperature effect on N_2O concentration was also observed in experiment N3. The SP values at both temperatures were almost nearby which have almost no temperature influence as well. This suggests N_2O production process was not significantly affected by the temperature difference of 7°C, although N_2O production rate can be increased. In experiment N3, notable increases in $\delta^{15}\text{N}^{\text{bulk}}$, $\delta^{18}\text{O}$, and SP observed between $t = 150$ and 210 min at 25°C were not found at 18°C, which indicates that N_2O reduction might have been promoted at higher temperatures. For experiments N2 and N4, unfortunately, it remains unclear how the concentration and isotopocule ratios of N_2O were changed because they were measured only at the beginning and end of the time course.

The difference in $\delta^{18}\text{O}$ - N_2O in N1 between 25°C and 18°C was approximately 10%. This fact might be explained by a different degree of O-exchange between NO_2^- and H_2O . The production rate of N_2O was lower at 18°C than at 25°C (Figs. 6a and 6e). Therefore, the O-exchange can be enhanced if the rate-limiting step is NO_2^- reduction. No report in the literature to date has described the temperature dependence of O-exchange rate during microbiological N_2O production. Further studies must be conducted to elucidate this point.

Source-partitioning of N₂O Here we discuss the N_2O production/consumption processes under a steady state as-

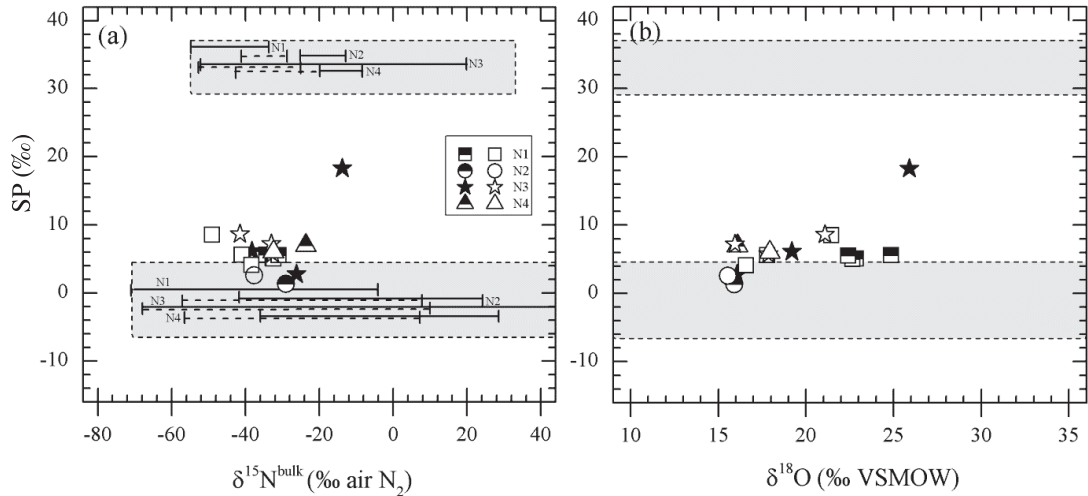


Fig. 9. Relation between SP and $\delta^{15}\text{N}^{\text{bulk}}$ and between SP and $\delta^{18}\text{O}$ of dissolved N_2O at 60–210 min during oxic experiments at both 25°C and 18°C. Gray rectangles show overall ranges for N_2O produced by nitrification (NH_2OH -oxidation, upper boxes) and by nitrifier-denitrification (NO_2^- reduction, bottom boxes). The ranges of $\delta^{15}\text{N}^{\text{bulk}}$ for each experiment (N1–N4) were estimated using Eq. (6); they are shown by horizontal capped segments with solid (25°C) and dashed (18°C) lines (a). The SP of N_2O produced by NH_2OH oxidation was assigned as 29–37‰, whereas those by NO_2^- reduction were $-1.0 \pm 5.5\%$. In (b), only the expected ranges of SP are shown by horizontal belts. The N_2O produced in each experiment is shown with closed/half-closed (25°C) and open (18°C) symbols.

suming that (i) N_2O production and its emission to the gas phase were balanced, (ii) N_2O reduction was sufficiently small, except at $t = 150\text{--}210$ min in experiment N3 at 25°C, and (iii) production processes were unchanged at $t = 60$ min or later. These assumptions are based on full time series measurements in experiments N1 and N3, although temporal variation of N_2O concentration and isotopocule ratios were not negligible in N3 at 25°C. We can regard the isotopocule ratios after 60 min as values for N_2O produced in the system because isotope fractionation associated with emission of dissolved N_2O to the gas phase is sufficiently small compared to that related to N_2O production (Inoue and Mook, 1994).

In Figs. 9a and 9b, the data obtained at $t = 60$ min or later are shown, respectively, in SP- $\delta^{15}\text{N}^{\text{bulk}}$ and SP- $\delta^{18}\text{O}$ diagrams. Experiments N1–N4 were conducted under oxic conditions. Therefore, N_2O should have been produced by NH_2OH oxidation (nitrification) or NO_2^- reduction (nitrifier-denitrification) pathways. The range of SP values for N_2O produced by NH_2OH oxidation (nitrification) or NO_2^- reduction (nitrifier-denitrification) is shown by the vertical sides of the gray rectangles in Figs. 9a and 9b. The resulting range of $\delta^{15}\text{N}^{\text{bulk}}$ for N_2O produced by NH_2OH oxidation in each experiment is shown by a horizontal capped segment in the upper gray rectangle in Fig. 9a (solid and dashed lines correspond to experiments conducted at 25°C and 18°C, respectively). $\delta^{15}\text{N}\text{-NO}_2^-$ was not measured individually in this study. Therefore, we

estimate $\delta^{15}\text{N}^{\text{bulk}}$ for N_2O produced by NH_4^+ oxidation to NO_2^- followed by NO_2^- reduction using $\delta^{15}\text{N}\text{-NH}_4^+$ and $\epsilon(^{15}\text{N})_{\text{NH}_4^+ \rightarrow \text{NO}_2^- \rightarrow \text{N}_2\text{O}}$. The $\epsilon(^{15}\text{N})_{\text{NH}_4^+ \rightarrow \text{NO}_2^- \rightarrow \text{N}_2\text{O}}$ is estimated from $\epsilon(^{15}\text{N})_{\text{NH}_4^+ \rightarrow \text{NO}_2^-}$ and $\epsilon(^{15}\text{N})_{\text{NO}_2^- \rightarrow \text{N}_2\text{O}}$ reported in the literature (−76 to −11‰, Toyoda *et al.*, 2011a). The range of $\epsilon(^{15}\text{N})_{\text{NH}_4^+ \rightarrow \text{N}_2\text{O}}$ obtained by studies incubating pure culture of nitrifying bacteria under aerobic conditions (−60 to −48‰, Toyoda *et al.*, 2011a) is assumed to represent ^{15}N -enrichment factor for N_2O production from NH_4^+ via NH_2OH . The calculated range of $\delta^{15}\text{N}^{\text{bulk}}$ for N_2O produced by NO_2^- reduction in each experiment is shown as a horizontal capped segment in the bottom gray rectangle in Fig. 9a. The SP values of measured N_2O in experiments N1–N4 with different DO concentrations at both temperatures (+5.0 – +5.6‰ at 25°C and +4.1 – +8.5‰ at 18°C) are close to the range of SP for NO_2^- reduction source. Observed SP values show that N_2O production in most of the oxic experiments is consistent with nitrifier-denitrification (Fig. 9a), which dominantly contributed to N_2O production as about 74–87% for experiment N1, 92–96% for experiment N2, 74–92% for experiment N3 and 79–82% for experiment N4, respectively, from Eq. (4). Our results agree with those from studies by Wunderlin *et al.* (2013), who found that nitrifier-denitrification was the dominant N_2O production process in an experiment exploring the multiple steps of NH_4^+ oxidation. This finding can also be confirmed by the progressive depletion of NH_4^+ and NO_2^- accumulation (Figs. 5a, 5c, 5d, and 5f). The SP values of N_2O observed in

experiments with low DO (N1 and N2) were close to the values obtained in experiment N3, which was conducted under reference conditions. This result suggests that the changes in DO did not alter the N₂O production pathway (NO₂⁻ reduction by AOB). However, high SP values were observed at 25°C in experiment N3 at 210 min (+18.3%). This is explainable by the partial contribution (*ca.* 55%) of N₂O produced via NH₂OH oxidation. Nevertheless, at least for N3, the N₂O reduction could also be the cause (see below).

The δ¹⁸O of N₂O produced either by NH₂OH oxidation or NO₂⁻ reduction by AOB is not well constrained to date. Although the δ¹⁸O also has process-dependent and substrate dependent signatures like δ¹⁵N^{bulk}, it is difficult to estimate the range of δ¹⁸O of N₂O produced by each process using an equation similar to Eq. (5) because several substrates are involved (e.g., O₂, H₂O, NO₂⁻). Moreover, ε(¹⁸O) for each production process has not been well characterized. Therefore we showed no range of δ¹⁸O of N₂O in Fig. 9b: the horizontal belt shows the range of SP for N₂O production process.

We found a significant correlation between SP and δ¹⁸O of N₂O during the “steady state” phase (*t* = 60 min or later) in experiment N3 at 25°C (slope 1.619, *R*² = 0.988, Fig. 6b). This might indicate that N₂O reduction happened to be enhanced during the “steady state”, because it is known that isotopocule ratios show co-variation during N₂O reduction (Table 3). However, no significant correlation was observed between δ¹⁵N^{bulk} and δ¹⁸O nor between δ¹⁵N^{bulk} and SP, and apparent correlation could be obtained not only N₂O reduction process but also mixing of different N₂O production processes. Further studies are needed to explore the temporal change in N₂O production/consumption processes using the concentration and isotopocule ratios.

CONCLUSION

We conducted batch incubation experiments using activated sludge under oxic and anoxic conditions to investigate the main factors underpinning N₂O production and consumption. Our results emphasize the usefulness of measurements of N₂O isotopocules together with the isotopic signature of NH₄⁺ and NO₃⁻ for identifying N₂O production and consumption mechanisms in a lab-scale simulation of biological wastewater treatment. Understanding of N₂O production mechanism which interpreted by these experiments can induce well management on the mitigation strategy of N₂O emission through effective ways to control key factors affecting N₂O production. The main findings obtained in this study are summarized as presented below.

- Under the condition in which N₂O production is negligible, increased concentration of MLSS enhances N₂O

reduction to N₂ in anoxic treatment. Enrichment factors (ε_R's) for N₂O reduction by activated sludge are first estimated as -9.5 ± 1.0‰ for δ¹⁵N^{bulk}, -28.7 ± 3.7‰ for δ¹⁸O and -10.0 ± 2.2‰ for SP.

- During N₂O reduction, strong linear relations were found between δ¹⁸O and δ¹⁵N^{bulk} with slope of 2.2, and between SP and δ¹⁵N^{bulk} with slope of 0.9. The slopes obtained in this study would be more applicable to the studies of N₂O dynamics in wastewater treatment than ε_R obtained from pure culture of denitrifying bacteria.

- N₂O production can be enhanced under decreased DO conditions during oxic treatment. However, the N₂O production mechanism is not sensitive to DO. Moreover, the nitrifier-denitrification by AOB during NH₄⁺ oxidation is the main pathway for N₂O production in most cases examined in this study.

- During anoxic treatment, N₂O is dominantly produced by NO₂⁻ reduction (heterotrophic denitrification); N₂O reduction to N₂ occurs simultaneously. The N₂O production mechanism is not sensitive to the temperature or the C/N ratio.

Acknowledgments—This work was partly funded by Global Environmental Research Fund (A-0904) of the Ministry of Environment, Japan and JSPS KAKENHI Grant Number 23224013. We thank the technical staff of the Bureau of Sewerage, Tokyo Metropolitan Government for sampling and analysis. We also thank three anonymous reviewers and S. Hattori for valuable comments on this manuscript. A. Tumendelger was supported by Global COE program “From the Earth to Earths” project of MEXT.

REFERENCES

- Barford, C. C., Montoya, J. P., Altabet, M. A. and Mitchell, R. (1999) Steady-state nitrogen isotope effects of N₂ and N₂O production in *Paracoccus denitrificans*. *Appl. Environ. Microbiol.* **65**, 989–994.
- Casciotti, K. L., Sigman, D. M., Hastings, M. G., Böhlke, J. K. and Hilkert, A. (2002) Measurement of the oxygen isotopic composition of nitrate in seawater and freshwater using the denitrifier method. *Anal. Chem.* **74**, 4905–4912.
- Chung, Y. C. and Chung, M. S. (2000) BNP test to evaluate the influence of C/N ratio on N₂O production in biological denitrification. *Water Sci. Technol.* **42**, 23–27.
- Colliver, B. B. and Stephenson, T. (2000) Production of nitrogen oxide and dinitrogen oxide by autotrophic nitrifiers. *Biotechnol. Adv.* **18**, 219–232.
- Coplen, T. B. (2011) Guidelines and recommended terms for expression of stable-isotope-ratio and gas-ratio measurement results. *Rapid Commun. Mass Spectrom.* **25**(17), 2538–2560.
- Fujii, A., Toyoda, S., Yoshida, O., Watanabe, S., Sasaki, K. and Yoshida, N. (2013) Distribution of nitrous oxide dissolved in water masses in the eastern subtropical North Pacific and its origin inferred from isotopomer analysis. *J. Oceanogr.* **69**(2), 147–157.

- Hanaki, K., Hong, Z. and Matsuo, T. (1992) Production of nitrous oxide gas during denitrification of wastewater. *Water Sci. Technol.* **26**, 1027–1036.
- Holmes, R. M., McClell, J. W., Sigman, D. M., Fry, B. and Peterson, B. J. (1998) Measuring $^{15}\text{N-NH}_4^+$ in marine, estuarine and freshwaters: An adaptation of the ammonia diffusion method for samples with low ammonium concentrations. *Mar. Chem.* **60**, 235–243.
- IPCC (2007) Climate Change 2007: synthesis report. Geneva, Switzerland.
- Inoue, H. Y. and Mook, W. G. (1994) Equilibrium and kinetic nitrogen and oxygen isotope fractionations between dissolved and gaseous N_2O . *Chem. Geol.* **113**, 135–148.
- Itokawa, H., Hanaki, K. and Matsuo, T. (1996) Nitrous oxide emission during nitrification and denitrification in a full-scale night soil treatment plant. *Water Sci. Technol.* **34**, 277–284.
- Itokawa, H., Hanaki, K. and Matsuo, T. (2001) Nitrous oxide production in high-loading biological nitrogen removal process under low COD/N ratio condition. *Water Res.* **35**, 657–664.
- Kampschreur, M. J., Tan, N. C. G., Kleerebezem, R., Picoreanu, C., Jetten, M. S. M. and van Loosdrecht, M. C. M. (2008) Effect of dynamic process conditions on nitrogen oxides emission from nitrifying culture. *Environ. Sci. Technol.* **42**, 429–435.
- Kampschreur, M. J., Temmink, H., Kleerebezem, R., Jetten, M. S. M. and van Loosdrecht, M. C. M. (2009) Nitrous oxide emission during wastewater treatment. *Water Res.* **43**, 4093–4103.
- Kim, K. R. and Graig, H. (1993) Nitrogen-15 and oxygen-18 characteristics of nitrous oxide: a global perspective. *Science* **262**, 1855–1857.
- Kimochi, Y., Inamori, Y., Mizuochi, M., Xu, K. and Matsumura, M. (1998) Nitrogen removal and N_2O emission in a full scale domestic wastewater treatment plant with intermittent aeration. *J. Ferm. Bioeng.* **86**, 202–206.
- Koba, K., Osaka, K., Tobar, Y., Toyoda, S., Ohte, N., Katsuyama, M., Suzuki, N., Itoh, M., Yamagishi, H., Kawasaki, M., Kim, S. J., Yoshida, N. and Nakajima, T. (2009) Biogeochemistry of nitrous oxide in groundwater in a forested ecosystem elucidated by nitrous oxide isotopomer measurements. *Geochim. Cosmochim. Acta* **73**, 3115–3133.
- Mariotti, A., Germon, J. C., Hubert, P., Kaiser, P., Le'olle, R., Tardieux, A. and Tardieux, P. (1981) Experimental determination of nitrogen kinetic isotope fractionation: some principles: illustration for the denitrification and nitrification processes. *Plant Soil.* **62**, 413–430.
- Noda, N., Kaneko, N., Mikami, M., Kimochi, Y., Tsuneda, S., Hirata, A., Mizuochi, M. and Inamori, Y. (2003) Effects of SRT and DO on N_2O reductase activity in an anoxic-oxic activated sludge system. *Water Sci. Technol.* **48**(11–12), 363–370.
- Ostrom, N. E., Pitt, A., Sutka, R., Ostrom, P. H., Grandy, A. S., Huizinga, K. M. and Robertson, G. P. (2007) Isotopologue effects during N_2O reduction in soils and in pure cultures of denitrifiers. *J. Geophys. Res.* **112**, G02005.
- Ravishankara, A. R., Daniel, J. S. and Portmann, R. W. (2009) Nitrous oxide (N_2O): The dominant ozone-depleting substance emitted in the 21st century. *Science* **326**, 123–125.
- Sigman, D. M., Casciotti, K. L., Andreani, M., Barford, C., Galanter, M. and Böhlke, J. K. (2001) A bacterial method for the nitrogen isotopic analysis of nitrate in seawater and freshwater. *Anal. Chem.* **73**, 4145–4153.
- Sutka, R. L., Ostrom, N. E., Ostrom, P. H., Gandhi, H. and Breznak, J. A. (2003) Nitrogen isotopomer site preference of N_2O produced by *Nitrosomonas europaea* and *Methylococcus capsulatus* Bath. *Rapid Commun. Mass Spectrom.* **17**, 738–745.
- Sutka, R. L., Ostrom, N. E., Ostrom, P. H., Gandhi, H. and Breznak, J. A. (2004) Nitrogen isotopomer site preference of N_2O produced by *Nitrosomonas europaea* and *Methylococcus capsulatus* Bath. *Rapid Commun. Mass Spectrom.* **18**, 1411–1412.
- Sutka, R. L., Ostrom, N. E., Ostrom, P. H., Breznak, J. A., Gandhi, H., Pitt, A. J. and Li, F. (2006) Distinguishing nitrous oxide production from nitrification and denitrification based on isotopomer abundances. *Appl. Environ. Microbiol.* **72**, 638–644.
- Tallec, G., Garnier, J., Billen, G. and Gossailles, M. (2006) Nitrous oxide emissions from secondary activated sludge in nitrifying conditions of urban wastewater treatment plants: effect of oxygenation level. *Water Res.* **40**, 2972–2980.
- Townsend-Small, A., Pataki, D. E., Tseng, L. Y., Tsai, C.-Y. and Rosso, D. (2011) Nitrous oxide emissions from water reclamation plants in southern California. *J. Environ. Qual.* **40**, 1542–1550.
- Toyoda, S. and Yoshida, N. (1999) Determination of nitrogen isotopomers of nitrous oxide on a modified isotope ratio mass spectrometer. *Anal. Chem.* **71**, 4711–4718.
- Toyoda, S., Mutobe, H., Yamagishi, H., Yoshida, N. and Tanji, Y. (2005) Fractionation of N_2O isotopomers during production by denitrifier. *Soil Biol. Biochem.* **37**, 1535–1545.
- Toyoda, S., Suzuki, Y., Hattori, S., Yamada, K., Fujii, A., Yoshida, N., Kouno, R., Murayama, K. and Shiomi, H. (2011a) Isotopomer analysis of production and consumption mechanisms of N_2O and CH_4 in an advanced wastewater treatment system. *Environ. Sci. Technol.* **45**, 917–922.
- Toyoda, S., Yano, M., Nishimura, S., Akiyama, H., Hayakawa, A., Koba, K., Sudo, S., Yagi, K., Makabe, A., Tobar, Y., Ogawa, N., Ohkouchi, N., Yamada, K. and Yoshida, N. (2011b) Characterization and production and consumption processes of N_2O emitted from temperate agricultural soils determined via isotopomer ratio analysis. *Global Biochem. Cycles* **25**, GB 2008.
- Toyoda, S., Koba, K. and Yoshida, N. (2015) Isotopologue analysis of biologically produced nitrous oxide in various environments. *Mass Spectrom. Rev.*, doi:10.1002/mas.21459.
- Tumendelger, A., Toyoda, S. and Yoshida, N. (2014) Isotopomer analysis of N_2O produced in a wastewater treatment system operated under standard activated sludge method. *Rapid Commun. Mass Spectrom.* **28**(17), 1883–1892.
- Waechter, H., Mohn, J., Tuzson, B., Emmenegger, L. and Sigrist, M. W. (2008) Determination of N_2O isotopomers absorption spectroscopy with quantum cascade laser based spectroscopy. *Opt. Express* **16**, 9239–9244.
- Weiss, R. F. and Price, B. A. (1980) Nitrous oxide solubility in

- water and seawater. *Mar. Chem.* **8**, 347–359.
- Wrage, N., Velthof, G. L., van Beusichem, K. L. and Oenema, O. (2001) Role of nitrifier denitrification in the production of nitrous oxide. *Soil Biol. Biochem.* **33**, 1723–1732.
- Wunderlin, P., Mohn, J., Joss, A., Emmenegger, L. and Siegrist, H. (2012) Mechanisms of N₂O production in biological wastewater treatment under nitrifying and denitrifying conditions. *Water Res.* **46**, 1027–1037.
- Wunderlin, P., Lehmann, M. F., Siegrist, H., Tuzson, B., Joss, A., Emmenegger, L. and Mohn, J. (2013) Isotope signatures of N₂O in a mixed microbial population system: Constraints on N₂O producing pathway in wastewater treatment. *Environ. Sci. Technol.* **47**, 1339–1348.
- Yamagishi, H., Westley, M. B., Popp, B. N., Toyoda, S., Yoshida, N., Watanabe, S., Koba, K. and Yamanaka, Y. (2007) Role of nitrification and denitrification on the nitrous oxide cycle in the eastern tropical North Pacific and Gulf of California. *J. Geophys. Res.* **112**, G02015.
- Yoshida, N. and Toyoda, S. (2000) Constraining the atmospheric N₂O budget from intramolecular site preference in N₂O isotopomers. *Nature* **405**, 330–334.
- Yoshida, N., Hattori, A., Saino, T., Matsuo, S. and Wada, E. (1984) ¹⁵N/¹⁴N ratio of dissolved N₂O in the eastern tropical Pacific Ocean. *Nature* **307**, 442–444.
- Yoshida, N., Morimoto, H., Hirano, M., Koike, I., Matsuo, S., Wada, E., Saino, T. and Hattori, A. (1989) Nitrification rates and ¹⁵N abundances of N₂O and NO₃⁻ in the western North Pacific. *Nature* **342**, 895–897.
- Yoshinari, T. and Wahlen, M. (1985) Oxygen isotope ratios in N₂O from nitrification at a wastewater treatment facility. *Nature* **317**, 349–350.
- Yoshinari, T., Altabet, M. A., Naqvi, S. W. A., Codispotti, L., Jayakumar, A., Kuhland, M. and Devol, A. (1997) Nitrogen and oxygen isotopic composition of N₂O from suboxic waters of the eastern tropical North Pacific and the Arabian Sea—Measurement by continuous-flow isotope-ratio monitoring. *Mar. Chem.* **56**, 253–264.
- Zheng, H., Hanaki, K. and Matsuo, T. (1994) Production of nitrous oxide gas during nitrification of wastewater. *Water Sci. Technol.* **30**, 133–141.